

Lawrence Berkeley National Laboratory

LBL Publications

Title

Critical Properties of Polydisperse Fluid Mixtures from an Equation of State

Permalink

<https://escholarship.org/uc/item/254494w5>

Authors

Cai, J

Liu, H

Hu, Y

et al.

Publication Date

1999-09-01

Copyright Information

This work is made available under the terms of a Creative Commons Attribution License, available at <https://creativecommons.org/licenses/by/4.0/>



ERNEST ORLANDO LAWRENCE BERKELEY NATIONAL LABORATORY

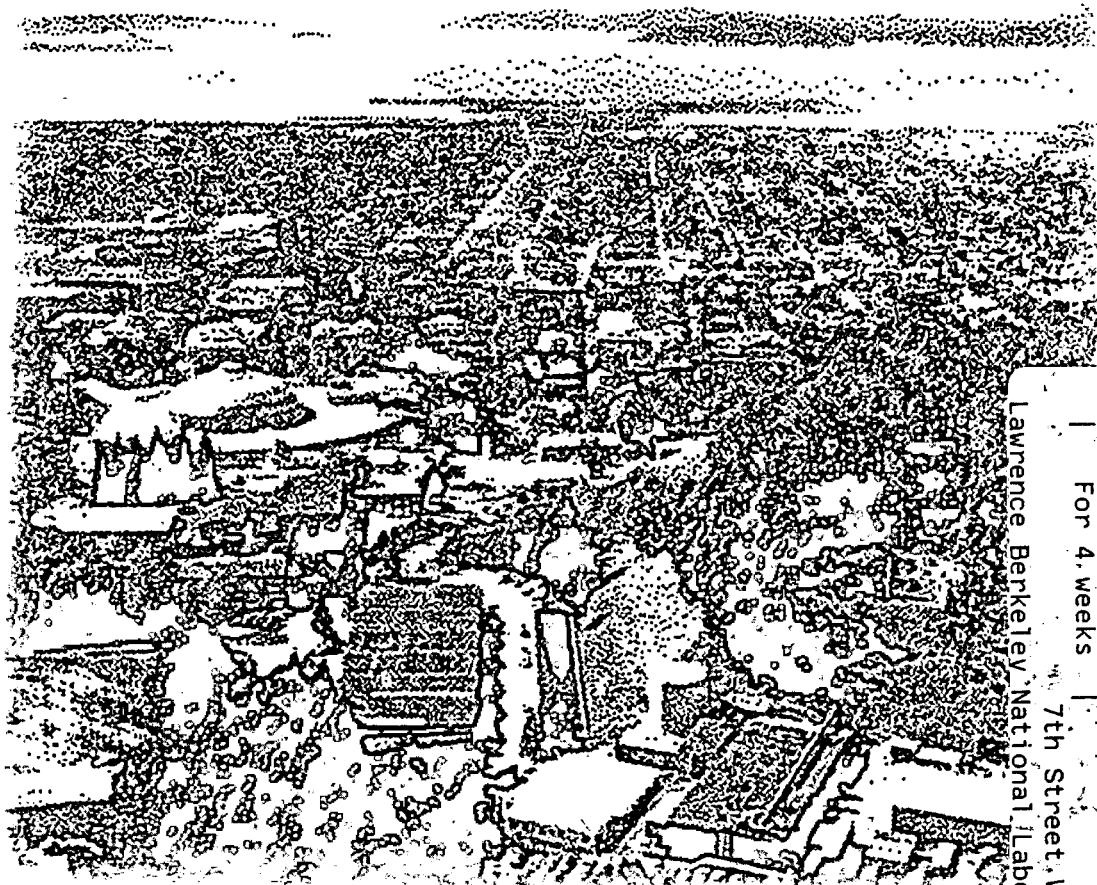
Critical Properties of Polydisperse Fluid Mixtures from an Equation of State

J. Cai, H. Liu, Y. Hu, and J.M. Prausnitz

Chemical Sciences Division

September 1999

Submitted to
Fluid Phase Equilibria



LOAN COPY
Circulates
For 4 weeks
7th Street Warehouse
Lawrence Berkeley National Laboratory
LBNL-44224
Copy 2

DISCLAIMER

This document was prepared as an account of work sponsored by the United States Government. While this document is believed to contain correct information, neither the United States Government nor any agency thereof, nor the Regents of the University of California, nor any of their employees, makes any warranty, express or implied, or assumes any legal responsibility for the accuracy, completeness, or usefulness of any information, apparatus, product, or process disclosed, or represents that its use would not infringe privately owned rights. Reference herein to any specific commercial product, process, or service by its trade name, trademark, manufacturer, or otherwise, does not necessarily constitute or imply its endorsement, recommendation, or favoring by the United States Government or any agency thereof, or the Regents of the University of California. The views and opinions of authors expressed herein do not necessarily state or reflect those of the United States Government or any agency thereof or the Regents of the University of California.

Critical Properties of Polydisperse Fluid Mixtures from an Equation of State

J. Cai, H. Liu, Y. Hu and J. M. Prausnitz

Department of Chemical Engineering

University of California

and

Chemical Sciences Division

Lawrence Berkeley National Laboratory

University of California

Berkeley, CA 94720, U.S.A.

September 1999

This work was supported by the Director, Office of Science, Office of Basic Energy Sciences, Chemical Sciences Division of the U.S. Department of Energy under Contract Number DE-AC03-76SF00098.

Critical Properties of Polydisperse Fluid Mixtures

from an Equation of State

Jun Cai ^a, Honlai Liu ^a, Ying Hu ^{a*} and John M. Prausnitz ^b

^a *Department of Chemistry, East China University of Science and Technology, Shanghai 200237, People's Republic of China*

^b *Department of Chemical Engineering, University of California, Berkeley and Chemical Sciences Division, Lawrence Berkeley National Laboratory, CA 94720, USA*

Abstract

Based on stability theory for polydisperse fluid mixtures, expressions have been developed for the spinodal criterion, critical criterion and various stability tests for systems containing one discrete component and one continuous homologue. Each criterion can be separated into two parts: the first part is the same in form as that for binary systems; when we assume particular mixing rules for parameters of the equation of state, that part is determined only by the average molar mass of the homologue. The second part is concerned with the distribution function that characterizes the continuous component. To illustrate results, the van der Waals equation of state is used to calculate critical properties; the composition dependences of parameters $a^{1/2}$ and b of the van der Waals equation are assumed to be linear functions of molar mass. Numerical results for the critical loci are obtained. For a discrete component i and a continuous component j , systematic variations of parameters in the distribution function for j or of the interaction parameter a_{ij} show transitions between qualitatively different types of phase behavior.

Keywords Continuous thermodynamics, critical point, spinodal, equation of state

1. Introduction

To understand the phase behavior of fluid mixtures, it is necessary to utilize a reliable method for calculating spinodals and critical points. Most published work has been limited to binaries; only a few studies have investigated ternaries. The phase-behavior classification widely adopted at present is due to van Konynenburg and Scott [1, 2]. They showed that the van der Waals equation, when applied to binary mixtures, predicted almost all observed types of phase behavior except type VI. Each of types I to V occupies a certain region in a two-dimensional global phase diagram where intermolecular interaction parameters are axes.

Van Konynenburg and Scott have inspired the systematic study of phase behavior by various equations of state. Furman et al [3, 4] studied the symmetric ternary lattice gas and the van der Waals lattice gas, and located some new types of phase behavior. Mazur [5] used Ree's equation to study Lennard-Jones fluids and to calculate the phase behavior of types VI and VII. Deiters and Pegg[6] used the Redlich-Kwong equation while Kraska and Deiters[7] used the Carnahan-Starling-Redlich-Kwong equation to calculate global phase diagrams. Pelt et al [8] adopted a simplified perturbed hard-chain equation; they were able to identify up to ten types. Nezebeda et al [9-14] investigated model binary mixtures consisting of associating components as well as Lorentz-Berthelot mixtures of attractive hard spheres.

Although recent work following the pioneering study of van Konynenburg and Scott concerning binary mixtures has achieved better understanding of binary and ternary phase behavior, we know little about the phase behavior of multicomponent systems. In polymer solutions and polymer blends, as well as in petroleum fractions, vegetable oils and other "natural" fluids, there are very many components. It is often not practical, indeed it may be impossible, to perform the chemical analysis to determine the exact compositions of such systems. At best, chemical analysis can provide some statistical properties, such as molar-mass distribution, normal-boiling-point distribution and so on. To calculate the thermodynamic properties of such ultramulticomponent systems, continuous thermodynamics

* Corresponding author

[15-17] has been developed; in continuous thermodynamics, a distribution function replaces the customary discrete composition variable.

For spinodals and critical points, we need stability criteria. For lattice models or their modifications, the stability criteria were successfully established for systems containing continuous components [18-22]. However, for equations of state, we remain at a beginning stage. Following Cotterman and Prausnitz [23], Kehlen et al [24] used a variation method while Hu and Ying [25] used a discrete-components method to establish the necessary stability criteria for systems containing one homologous series whose properties are described by an equations of state. Later, Hu and Prausnitz [26] developed comprehensive stability criteria for systems containing an arbitrary number of discrete components and an arbitrary number of homologous series for both the lattice and the equations-of-state models. Using a discrete-components method, they introduced two theorems that can simplify the derivation of stability criteria for continuous systems. That work laid the foundation of calculations for critical properties of polydisperse fluid mixtures; however, no numerical illustrations were provided. Recently, Browarzik and Kehlen [27] obtained the stability criteria for systems containing one discrete component and one continuous homologous series using a variation method without performing stability tests; only a few numerical results are presented and these appear to be restricted to type I.

This work also concerns the critical properties for polydisperse systems containing one discrete component and one continuous homologous series but, unlike Browarzik and Kehlen, stability tests are included. Based on our previous work [26], the derivation of stability criteria is reconsidered to yield new expressions that are both simpler and in a more reasonable form. Stability tests for discrete multicomponent systems based on Heidemann's work [28] are here applied to a continuous system. The important results of this work are relations that give the transition between various types of phase behavior, mainly types I to V. While the illustrative calculations reported here use the van der Waals equation of state, any other equation of state could be used to reduce our general results to practice.

2. Theoretical Framework

We consider a system that contains one solvent and one polydisperse homologue (a homologous series); the latter has $K-1$ components where K approaches infinity. The molar Helmholtz function of the system can be expressed by

$$A_m = \sum_{i=1}^K x_i (A_{m,i}^0 + RT \ln x_i) + A_m^r(T, V_m, a, b, c) = A_m^{\text{id}} + A_m^r \quad (1)$$

where $A_{m,i}^0$, A_m^r and A_m^{id} are, respectively, the standard molar Helmholtz function of the i th component, the residual molar Helmholtz function of the mixture and the molar Helmholtz function of the ideal mixture. The solvent is defined as the K th component. The equation of state contains parameters a, b, c that can be expressed by

$$a = a(T, x\bar{M}, x) \quad , \quad b = b(T, x\bar{M}, x) \quad , \quad c = c(T, x\bar{M}, x) \quad (2)$$

where x and \bar{M} are the total mole fraction and the average molar mass of the homologue, respectively:

$$x = \sum_{i=1}^{K-1} x_i \quad (3)$$

$$x\bar{M} = \sum_{i=1}^{K-1} x_i M_i \quad (4)$$

Eq.(4) can be extended to include any arbitrary-order moment of molar mass.

2.1 Spinodal Criterion

As shown previously [26], on the spinodal surface, the 2nd-order variation of the molar Helmholtz function can be expressed by

$$\begin{aligned} \delta^{(2)} A_m = & \sum_{i=1}^{K-1} \sum_{j=1}^{K-1} \frac{\partial^2 A_m^{\text{id}}}{\partial x_i \partial x_j} \delta x_i \delta x_j + A_{MM}^r (\delta x \bar{M})^2 + A_{xx}^r (\delta x)^2 + A_{V^r}^r (\delta V_m)^2 \\ & + 2 A_{Mx}^r \delta x \bar{M} \delta x + 2 A_{VM}^r \delta V_m \delta x \bar{M} + 2 A_{Vx}^r \delta V_m \delta x \end{aligned}$$

$$\begin{aligned}
&= \sum_{i=1}^K j_i (\delta x_i)^2 + A_{MM}^r (\delta x \overline{M})^2 + A_{xx}^r (\delta x)^2 + A_{VV}^r (\delta V_m)^2 \\
&\quad + 2A_{Mx}^r \delta x \overline{M} \delta x + 2A_{VM}^r \delta V_m \delta x \overline{M} + 2A_{Vx}^r \delta V_m \delta x
\end{aligned} \tag{5}$$

where A_{VV}^r , A_{VM}^r , A_{Vx}^r , A_{MM}^r , A_{Mx}^r , A_{xx}^r are, respectively, the 2nd-order partial derivatives of A_m^r with respect to V_m , $x\overline{M}$ and x , $j_i = RT/x_i$. Variations of x and $x\overline{M}$ as well as higher-order moments satisfy the following conditions:

$$\sum_{i=1}^K \delta x_i = 0 \tag{6}$$

$$\sum_{i=1}^{K-1} M_i^n \delta x_i = \delta x \overline{M}^n, \quad n = 1, \dots, \infty \tag{7}$$

where

$$\overline{xM}^n = \sum_{i=1}^{K-1} x_i M_i^n, \quad n = 1, \dots, \infty \tag{8}$$

From our previous work [26], we have the following two relations:

$$\frac{\partial(\delta^{(2)} A_m)}{\partial(\delta V_m)} = 0 \tag{9}$$

$$\frac{\partial(\delta^{(2)} A_m)}{\partial(\delta x_i)} = 0, \quad i = 1, \dots, K-1 \tag{10}$$

Substituting eq.(5) into eqs.(9) and (10), multiplying eq.(10) by x_i and $x_i M_i$, respectively, summing all these equations from $i = 1$ to $K-1$, and utilizing the conditions set by eqs.(6) and (7), we obtain a homogeneous linear system of equations,

$$\begin{bmatrix}
A_{VV}^r & A_{Vx}^r & A_{VM}^r \\
A_{Vx}^r + \overline{M} A_{VM}^r & j_c + j_K + A_{xx}^r + \overline{M} A_{Mx}^r & A_{Mx}^r + \overline{M} A_{MM}^r \\
\mu_{(2)} A_{VM}^r & -j_c \overline{M} + \mu_{(2)} A_{Mx}^r & j_c + \mu_{(2)} A_{MM}^r
\end{bmatrix}
\begin{bmatrix}
\delta V_m \\
\delta x \\
\delta x \overline{M}
\end{bmatrix}
= \begin{bmatrix}
0 \\
0 \\
0
\end{bmatrix} \tag{11}$$

where $\mu_{(2)} = \overline{M^2} - \overline{M}^2$ is the variance of the distribution; $j_c = RT/x$, $j_K = RT/(1-x)$.

The sufficient and necessary condition for which the system of equations has a nontrivial solution is:

$$F_{sp}^r = \begin{vmatrix} A_{VV}^r & A_{Vx}^r & A_{VM}^r \\ A_{Vx}^r + \overline{M}A_{VM}^r & j_c + j_K + A_{xx}^r + \overline{M}A_{Mx}^r & A_{Mx}^r + \overline{M}A_{MM}^r \\ \mu_{(2)}A_{VM}^r & -j_c\overline{M} + \mu_{(2)}A_{Mx}^r & j_c + \mu_{(2)}A_{MM}^r \end{vmatrix} = 0 \quad (12)$$

This is the spinodal criterion equivalent to our previous result [26].

Eq.(12) can be expressed in another way:

$$F_{sp}^r = \begin{vmatrix} A_{VV}^r & A_{Vx}^r \\ A_{Vx}^r & j_c + j_K + A_{xx}^r \end{vmatrix} + \frac{x\mu_{(2)}}{RT} E \quad (13)$$

where

$$E = \begin{vmatrix} A_{VV}^r & A_{VM}^r & A_{Vx}^r \\ A_{VM}^r & A_{MM}^r & A_{Mx}^r \\ A_{Vx}^r & A_{Mx}^r & j_c + j_K + A_{xx}^r \end{vmatrix} \quad (14)$$

Subscript X in eq.(13) represents the total derivative with respect to x . For example, from eq.(2), the total derivative of parameter a in the van der Waals equation with respect to x is

$$\frac{Da(x, x\overline{M})}{Dx} = \frac{\partial a}{\partial x} + \frac{\partial a}{\partial x\overline{M}} \frac{\partial x\overline{M}}{\partial x} = \frac{\partial a}{\partial x} + \overline{M} \frac{\partial a}{\partial x\overline{M}} \quad (15)$$

Eq.(13) is useful because it separates the spinodal criterion into two parts. The first part (the determinant) is formally the same as the spinodal criterion of a binary mixture where the homologue is regarded as one component. The second part concerns the distribution function of the homologue. If the distribution function is a δ -function (a single component), \overline{M} is then a constant, $\mu_{(2)} = 0$, and eq.(13) reduces to the spinodal criterion for a binary mixture [24]. In that case, the total derivative (e. g. eq.(15)) reduces to the derivative with respect to mole fraction.

We write eq(13) in a more concise form:

$$F_{sp}^r = F_{sp}^{\text{dis}} + \frac{x\mu_{(2)}}{RT} E \quad (16)$$

where F_{sp}^{dis} is the determinant in the right-hand side of eq.(13).

2.2 Critical Criterion

The critical criterion can be obtained from the variation of the spinodal equation, i.e., eq.(12) or (13) or (16) [26],

$$\delta F_{\text{sp}} = \frac{\delta F_{\text{sp}}}{\delta V_m} \delta V_m + \frac{\delta F_{\text{sp}}}{\delta x} \delta x + \frac{\delta F_{\text{sp}}}{\delta x \bar{M}} \delta x \bar{M} + \frac{\delta F_{\text{sp}}}{\delta x \bar{M}^2} \delta x \bar{M}^2 = 0 \quad (17)$$

Dividing by δV_m , we have

$$\frac{\delta F_{\text{sp}}}{\delta V_m} = \frac{\delta F_{\text{sp}}}{\delta V_m} + \frac{\delta F_{\text{sp}}}{\delta x} \frac{\delta x}{\delta V_m} + \frac{\delta F_{\text{sp}}}{\delta x \bar{M}} \frac{\delta x \bar{M}}{\delta V_m} + \frac{\delta F_{\text{sp}}}{\delta x \bar{M}^2} \frac{\delta x \bar{M}^2}{\delta V_m} = 0 \quad (18)$$

Ratios between δx , $\delta x \bar{M}$ and δV_m can be obtained from equation (11). After some algebra, we have the following three equations:

$$\left\{ \begin{array}{l} A_{VV}^r + A_{Vx}^r \frac{\delta x}{\delta V_m} + A_{VM}^r \frac{\delta x \bar{M}}{\delta V_m} = 0 \\ A_{Vx}^r + \bar{M} A_{VM}^r + (j_c + j_K + A_{xx}^r + \bar{M} A_{Mx}^r) \frac{\delta x}{\delta V_m} + (A_{Mx}^r + \bar{M} A_{MM}^r) \frac{\delta x \bar{M}}{\delta V_m} = 0 \\ \mu_{(2)} A_{VM}^r + (-j_c \bar{M} + \mu_{(2)} A_{Mx}^r) \frac{\delta x}{\delta V_m} + (j_c + \mu_{(2)} A_{MM}^r) \frac{\delta x \bar{M}}{\delta V_m} = 0 \end{array} \right. \quad (19)$$

From these three equations, we can have three different pairs of solutions for $\delta x / \delta V_m$ and $\delta x \bar{M} / \delta V_m$. In our previous work [26], we arbitrarily chose one of them to show the derivation procedure. However, to obtain reasonable results, the choice is crucial. Only one solution pair can be used.

$$\frac{\delta x}{\delta V_m} = \frac{-A_{VM}^r (A_{Vx}^r + \bar{M} A_{VM}^r) + A_{VV}^r (A_{Mx}^r + \bar{M} A_{MM}^r)}{-A_{Vx}^r (A_{Mx}^r + \bar{M} A_{MM}^r) + A_{VM}^r (j_c + j_K + A_{xx}^r + \bar{M} A_{Mx}^r)} \quad (20)$$

$$\frac{\delta x \bar{M}}{\delta V_m} = \frac{-A_{VV}^r (j_c + j_K + A_{xx}^r + \bar{M} A_{Mx}^r) + A_{Vx}^r (A_{Vx}^r + \bar{M} A_{VM}^r)}{-A_{Vx}^r (A_{Mx}^r + \bar{M} A_{MM}^r) + A_{VM}^r (j_c + j_K + A_{xx}^r + \bar{M} A_{Mx}^r)} \quad (21)$$

To select the correct pair, we use the criterion that, when the Dirac δ function is used as a distribution function, i.e., when the mixture is a binary, the critical criterion derived should reduce to that for binaries. Only one pair can meet this boundary condition. The other pairs cannot recover the binary limit.

For the ratio $\overline{\delta x M^2} / \delta V_m$, multiplying eq.(10) by $x_i M_i^2$, summing from $i = 1$ to $K-1$ and utilizing eq.(7), we have:

$$\eta A_{VM}^r + (-j_c \overline{M} + \eta A_{Mx}^r) \frac{\delta x}{\delta V_m} + \eta A_{MM}^r \frac{\overline{\delta x M}}{\delta V_m} + j_c \frac{\overline{\delta x M^2}}{\delta V_m} = 0 \quad (22)$$

where $\eta = \overline{M^3} - \overline{M^2} \overline{M}$. Substituting eqs.(20), (21) into eq.(22), we obtain for the ratio $\overline{\delta x M^2} / \delta V_m$:

$$\frac{\overline{\delta x M^2}}{\delta V_m} = \frac{-\overline{M^2} [A_{VM}^r (A_{Vx}^r + \overline{M} A_{VM}^r) - A_{VV}^r (A_{Mx}^r + \overline{M} A_{MM}^r)] + x \eta E / RT}{-A_{Vx}^r (A_{Mx}^r + \overline{M} A_{MM}^r) + A_{VM}^r (j_c + j_K + A_{xx}^r + \overline{M} A_{Mx}^r)} \quad (23)$$

Now we have all the necessary ratios. Substituting eqs.(20), (21) and (23) into eq.(18), we obtain the critical criterion:

$$F_{cr} = \left| \frac{A_{VV}^r}{\partial F_{sp}^{dis}} \quad \frac{A_{Vx}^r}{DF_{sp}^{dis}} \right| + \frac{x \mu^{(2)}}{RT} \left| \frac{A_{VV}^r}{\partial E} \quad \frac{A_{Vx}^r}{DE} \right| + \frac{\mu^{(2)}}{RT} E + \frac{x \mu^{(2)}}{RT} \begin{vmatrix} A_{VV}^r & A_{VM}^r & A_{Vx}^r \\ A_{VM}^r & A_{MM}^r & A_{Mx}^r \\ \frac{\partial F_{sp}}{\partial V} & \frac{\partial F_{sp}}{\partial x M} & \frac{\partial F_{sp}}{\partial x} \end{vmatrix} \\ + \frac{x(\overline{M^2}^2 - \overline{M^3} \overline{M})}{RT} (A_{VV}^r A_{MM}^r - A_{VM}^r{}^2) E + \frac{x \eta}{RT} (A_{Vx}^r A_{VM}^r - A_{VV}^r A_{Mx}^r) E \quad (24)$$

Similar to the spinodal criterion eq.(13), eq.(24) is also separated into two parts. The first term is formally the same as that for a binary mixture. The other terms are concerned with the continuous distribution function that replaces the discrete composition variable. If the distribution function is a Dirac δ -function, $\mu^{(2)}$, η and $(\overline{M^2}^2 - \overline{M^3} \overline{M})$ all vanish; eq.(24) then reduces to the critical criterion for a binary mixture.

2.3 Stability Test

The roots of eqs.(13) and (24) are not necessarily the critical points of the system. To locate critical points, three stability criteria must also be satisfied [28].

(1) Mechanical stability:

$$p > 0, A_{VV} \geq 0 \quad (25)$$

(2) Local diffusion stability:

$$F_4 = \frac{\delta F_{cr}}{\delta V_m} = \frac{\delta F_{cr}}{\delta V_m} + \frac{\delta F_{cr}}{\delta x} \frac{\delta x}{\delta V_m} + \frac{\delta F_{cr}}{\delta x M} \frac{\delta x M}{\delta V_m} + \frac{\delta F_{cr}}{\delta x M^2} \frac{\delta x M^2}{\delta V_m} + \frac{\delta F_{cr}}{\delta x M^3} \frac{\delta x M^3}{\delta V_m} > 0. \quad (26)$$

If eq.(26) is equal to zero, a higher-order critical point is likely. In general, if $F_2 = \dots = F_{2n} = F_{2n+1} = 0$ and $F_{2n+2} > 0$, where $n \geq 1$, there exists an n th-order critical point. In this case, the higher-order variation of Helmholtz function must be calculated. The n th-order variation of Helmholtz function is given by:

$$F_n = \frac{\delta F_{n-1}}{\delta V_m} = \frac{\delta F_{n-1}}{\delta V_m} + \sum_{i=0}^{n-1} \frac{\delta F_{n-1}}{\delta x M^i} \frac{\delta x M^i}{\delta V_m} \quad (27)$$

where the ratio $\delta x M^i / \delta V_m$ is obtained in a similar manner. Multiplying eq.(10) by $x_j M_j^i$, summing from 1 to $K-1$, and utilizing eq.(7), we have:

$$j_c \frac{\delta x M^i}{\delta V_m} = -A_{VM}^r (M^{i+1} - M^i M) - A_{MM}^r (M^{i+1} - M^i M) \frac{\delta x M}{\delta V_m} + \left[j_c M^i - A_{Mx}^r (M^{i+1} - M^i M) \right] \frac{\delta x}{\delta V_m} \quad (28)$$

(3) Global diffusion stability:

$$(1-y) \left[\mu_K(T^c, p^c, y; f_t) - \mu_K^c(T^c, p^c, x; f) \right] + y \int f(I) \left[\mu_I(T^c, p^c, y; f_t) - \mu_I^c(T^c, p^c, x; f) \right] dI > 0 \quad (29)$$

where T^c and p^c are the roots of eqs.(13) and (24), μ_K and μ_I are the chemical potential of the discrete and the continuous component, respectively, x, f are mole fraction and the distribution function of the homologue for the system of interest, respectively; and y, f_t are mole fraction and distribution function of the homologue for the arbitrarily selected testing system, respectively. Mole fraction y and distribution function $f_t(I)$ must satisfy the conditions that $0 < y < 1$; $\int f_t(I) dI = 1$; $f_t(I) \geq 0$, where I is a distribution variable such as

molar mass. If there exists a value of y and a form of $f_t(I)$ such that eq.(29) is not satisfied while eqs.(25) and (26) are valid, then roots T^c and p^c are not the correct critical point because they probably describe a metastable state. It is impractical to test all possible forms of $f_t(I)$. In calculations reported here, we use only the distribution $f(I)$ identical to that of the system and try various values of y . The results are the same as those when we test with other distribution functions.

3. Illustrative Results Using the van der Waals Equation

Our goal is to examine the influence of polydispersity on critical properties of multicomponent mixtures. For simplicity, we adopt the van de Waals equation of state:

$$p = RT / (V_m - b) - a / V_m^2 \quad (30)$$

where V_m is the molar volume of the mixture and a and b depend on composition. The corresponding molar Helmholtz function is:

$$\begin{aligned} A_m = & (1-x)A_{m,K}^0 + x \int [A_m^0(I) + RT \ln(\Delta I)] f(I) dI + xRT \int f(I) \ln f(I) dI \\ & + (1-x)RT \ln(1-x) + xRT \ln x + RT \ln \frac{V_m^0}{V_m - b} + \frac{a}{b} \ln \frac{V_m}{V_m + b} \end{aligned} \quad (31)$$

For illustration, we represent the composition of the homologue by a beta-distribution in the region $I_{\min} \leq I \leq I_{\max}$, where I is a distribution variable such as molar mass and I_{\min} and I_{\max} are boundary values:

$$f(I, \alpha, \beta) = \frac{1}{(I_{\max} - I_{\min})B(\alpha, \beta)} \left(\frac{I - I_{\min}}{I_{\max} - I_{\min}} \right)^{\alpha-1} \left(\frac{I_{\max} - I}{I_{\max} - I_{\min}} \right)^{\beta-1} \quad (32)$$

where $B(\alpha, \beta)$ is the beta function, α and β are parameters determined by the average reduced molar mass and the variance. (In the following, we simply use $f(I)$ instead of $f(I, \alpha, \beta)$ for abbreviation.) For the illustrative purposes of this work, we set $I_{\min} = 16$ and $I_{\max} = 200 \text{g}\cdot\text{mol}^{-1}$. To relate van der Waals “constants” a and b to composition, we follow the procedure of Cotterman and Prausnitz [23]. Assuming that binary interaction parameters

k_d between solvent and homologue are constant and those between various components of the homologue are zero, the composition dependences of van der Waals parameters a and b are:

$$a = a_K(1-x)^2 + 2\sum_{i=1}^K x(1-x)(1-k_d) \int \sqrt{a_K a(I)} f(I) dI + x^2 \iint \sqrt{a(I)a(J)} f(I)f(J) dI dJ \quad (33)$$

$$b = (1-x)b_K + x \int b(I) f(I) dI \quad (34)$$

where a_K and b_K are van der Waals parameters for pure component K while $a(I)$ and $b(I)$ are van der Waals parameters for the homologue:

$$\sqrt{a(I)} = a^{(0)} + a^{(1)} I \quad (35)$$

$$b(I) = b^{(0)} + b^{(1)} I \quad (36)$$

where $a^{(0)}$, $a^{(1)}$, $b^{(0)}$ and $b^{(1)}$ are selected in a manner similar to that described by Cotterman and Prausnitz [23]. Substituting eqs.(35) and (36) into eqs.(33) and (34), we have

$$a = a_K(1-x)^2 + 2\sum_{i=1}^K (1-x)x(1-k_d) \sqrt{a_K} (a^{(0)} + a^{(1)} \bar{M}) + x^2 (a^{(0)} + a^{(1)} \bar{M})^2 \quad (37)$$

$$b = b_K(1-x) + x(b^{(0)} + b^{(1)} \bar{M}) \quad (38)$$

The derivatives of a and b with respect to x and $x\bar{M}$ are shown below. The unlisted higher-order derivatives are equal to zero.

$$\frac{\partial a}{\partial x} = -2a_K(1-x) + 2\sqrt{a_K} [a^{(0)}(1-2x) - a^{(1)}x\bar{M}](1-k_d) + 2xa^{(0)}(a^{(0)} + a^{(1)}\bar{M}) \quad (39)$$

$$\frac{\partial a}{\partial x \bar{M}} = 2\sqrt{a_K} a^{(1)}(1-x)(1-k_d) + 2xa^{(1)}(a^{(0)} + a^{(1)}\bar{M}) \quad (40)$$

$$\frac{\partial^2 a}{\partial x^2} = 2[a_K - 2a^{(0)}\sqrt{a_K}(1-k_d) + a^{(0)2}] \quad (41)$$

$$\frac{\partial^2 a}{\partial x \overline{M}^2} = 2a^{(1)} \quad (42)$$

$$\frac{\partial^2 a}{\partial x \partial x \overline{M}} = -2a^{(1)} \sqrt{a_K} (1 - k_d) + 2a^{(0)} a^{(1)} \quad (43)$$

$$\frac{\partial b}{\partial x} = b^{(0)} - b_K \quad (44)$$

$$\frac{\partial b}{\partial x \overline{M}} = b^{(1)} \quad (45)$$

4. Numerical Results

We use the numerical algorithm based on a one-dimensional search suggested by Hicks and Young [29] for obtaining the roots. The stability test is performed soon after obtaining the roots of eqs.(13) and (24). Discontinuity of the critical loci is a result of stability testing. In the figures to follow, unstable and metastable curves are not shown. We are concerned with the influence of the distribution of the continuous homologue on the transition between different types of phase behavior. The computer program was first tested by comparing binary results (using a Dirac δ function for the distribution) with those reported by van Konynenburg and Scott [1, 2].

4.1 Transition between Types II, III and IV

Fig. 1 shows the transition from type II to type III with increasing average molar mass of the homologue while keeping the variance unchanged, $\mu_{(2)} = 347 \text{ g}^2 \cdot \text{mol}^{-2}$. Reduced parameters are defined with respect to the corresponding properties of discrete component K , i.e., $p_r = p/p_K^c$ and $T_r = T/T_K^c$. Fig. 1(a) shows typical critical loci of type II, where average molar mass of the homologue $\overline{M} = 72 \text{ g} \cdot \text{mol}^{-1}$. The left nearly-vertical curve terminates at the UCEP (upper critical end point), the highest temperature of the UCST (upper critical solution temperature). C is the critical point of the pure discrete component. Fig. 1(b)

shows a state intermediate between type II and type III, where average molar mass increased to $\overline{M}=81.4 \text{ g}\cdot\text{mol}^{-1}$. Fig. 1(c) exhibits type III phase behavior, indicating that the transition is completed when average molar mass of the homologue increased to $\overline{M}=81.4 \text{ g}\cdot\text{mol}^{-1}$.

Next we fix the average molar mass of the homologue, $\overline{M}=96 \text{ g}\cdot\text{mol}^{-1}$, and change the variance. Fig. 2 shows critical loci for a binary with $\mu_{(2)}=0$. The critical loci are separated into three branches indicating typical type IV phase behavior; C is the critical point of pure component K. Fig. 3 shows the influence of increasing variance. To show our results more clearly, we enlarge the region near point C. Fig. 3 shows that, upon increasing the variance from $\mu_{(2)}=0$ to 35 to $80 \text{ g}^2\cdot\text{mol}^{-2}$, phase behavior transforms from type IV to type III. Fig. 5 shows the distribution function for the homologue corresponding to Fig. 3.

Fig.5 shows the influence of the variance with the average molar mass unchanged. In Fig. 5, we use the same parameters as those in Fig. 3 except that interaction parameter $k_d=-0.1267$ (for Fig. 3, $k_d=-0.1723$). Also, $a^{(1)}$ is slightly changed to initiate the expected transition. Fig. 5 shows that, when the variance increases from $\mu_{(2)}=0$ to 347 to $800 \text{ g}^2\cdot\text{mol}^{-2}$ ($\overline{M}=96 \text{ g}\cdot\text{mol}^{-1}$), the phase behavior transforms from type II to type IV. Fig. 6 enlarges the loci near the critical point of pure solvent C. Fig.6 clearly shows splitting of a continuous locus into two branches.

Fig. 7 is an extension of Fig. 1 where we increase the average molar mass with the variance unchanged. Parameters are the same as those in Fig.1 except that $T_K^c=600\text{K}$ (400K in Fig. 1), $\mu_{(2)}=800 \text{ g}^2\cdot\text{mol}^{-2}$ ($\mu_{(2)}=347 \text{ g}^2\cdot\text{mol}^{-2}$ in Fig.1) and $k_d=-0.1267$ (-0.1067 in Fig. 1). Fig. 7 shows that when the average molar mass increases from $\overline{M}=72$ to 96, 104 and $112\text{g}\cdot\text{mol}^{-1}$, the phase behavior transforms from type II to type IV, then to type III. Fig. 8 shows the corresponding distribution functions for the continuous component.

4.2 Transition between Type I and Type V

It is well known that phase behavior of types I and V is similar to that of types II and IV except that in the former, there is no UCST curve. Figure 9 shows the transition from type I to type V with increase of the variance while keeping the average molar mass of the homologue unchanged, $\overline{M}=96\text{g}\cdot\text{mol}^{-1}$. All parameters are the same as those of Fig. 5 except $k_d = -0.207$. Fig. 10 shows an enlargement of the region near the critical point of pure solvent C. Fig.10 shows how a continuous locus (type I) splits into two branches (type V) when the variance increases from $\mu_{(2)}=0$ to 100, 147 and $600\text{g}^2\cdot\text{mol}^{-2}$.

5. Conclusions

We have presented a preliminary survey regarding the influence of the distribution function of a continuous component on the phase behavior of polydisperse fluid mixtures. Although our previous work established the foundation for derivation of expressions for spinodal and critical criteria, primary attention here has been given to calculation of critical properties. Special attention must be paid to the choice of reasonable expressions for ratios between variations δx , $\delta x\overline{M}$ and δV_m . Our essential criterion for this choice is that the expressions must reduce to the correct expression for a binary when a Dirac δ function is used for the distribution function for the composition of the homologue.

Because we adopt here the simple van der Waals equation, and because we assume a simple linear relation for equation-of-state parameters with respect to molar mass, our calculated phase behavior is similar to that reported by van Konynenburg and Scott for binaries. All five types, I, II, III, IV and V, were found. We investigated transition from one type to another through changes in the equation-of-state parameters and through changes in the distribution-function parameters. Generally, transitions only occur between types II, III and IV or between types I and V. Types I and V cannot transform to types II, III and IV or vice versa. Some preliminary rules are obtained: greater variance or greater average molar mass is favorable for types III, IV and V, while smaller variance or smaller average molar mass is favorable for types I and II. However, the type of phase behavior also depends on the equation-of-state parameters, especially on the interaction parameter that represents departure

from the geometric-mean assumption for estimating the interaction between the discrete component and the continuous component.

Acknowledgment This work was supported by the Chinese National Science Foundation and the Doctoral Research Foundation by the Ministry of Education of China. Additional support was provided by the Director, Office of Energy Research, Office of Basic Energy Science, Chemical Science Division of the U.S. Department of Energy under Contract No. DE-AC03-76SF0098.

List of Symbols

A Helmholtz function, J

a, b, c parameters of equation of state

$a^{(0)}, a^{(1)}, b^{(0)}, b^{(1)}$ parameters for determining the molar-mass dependence of a and b

D total derivative with respect to mole fraction

f distribution function

F stability criterion

I distribution variable such as molar mass

k_d solvent-homologue interaction parameter

\overline{M} average molar mass of the homologue, gmol^{-1}

\overline{M}^n n th-order moment of molar mass of the homologue (gmol^{-1}) n

R gas constant, $\text{Jmol}^{-1}\text{K}^{-1}$

T temperature, K

V volume, m^3

x, y mole fraction

α, β parameters of the distribution function

B Beta-function

η distribution parameter for the homologue

μ chemical potential

$\mu_{(2)}$ variance

subscripts

c continuous

K discrete component

m molar property

V, M, x derivative with respect to $V_m, x\bar{M}, x$

n n th-order variation

t testing system

superscripts

0 thermodynamic standard state

c critical

id ideal mixture

r residual

Literature Cited

1. R. L. Scott and P. H. van Konynenburg, *Discuss. Faraday Soc.*, **49** (1970) 87-97.
2. P. H. van Konynenburg and R. L. Scott, *Phil. Trans.*, **A 298** (1980) 495-540.
3. D. Furman, S. Dattagupta and R. B. Griffiths, *Phys. Rev. B* **15** (1977) 441-464.
4. D. Furman, S. Dattagupta and R. B. Griffiths, *Phys. Rev. A* **17**(1978)1139-
5. V. A. Mazur, L. Z. Boshkov and V. G. Murakhovsky, *Phys. Lett.* **104** (1984) 415-518.
6. U. K. Deiters and I. L. Pegg, *J. Chem. Phys.* **90** (1989) 6632-6641.
7. T. Kraska and U. K. Deiters, *J. Chem. Phys.* **96** (1991) 539-547.

8. A. van Pelt and T. W. de Loos, *J. Chem. Phys.* **97** (1992) 1271-1281.
9. I. Nezbeda, W. R. Smith and J. Kolafa, *J. Chem. Phys.* **100** (1994) 2191-2201.
10. I. Nezbeda, J. Kolafa, J. Pavlicek and W. R. Smith, *J. Chem. Phys.* **102** (1995) 638-9646.
11. I. Nezbeda, J. Kolafa and W. R. Smith, *Fluid Phase Equilibria*, **130** (1997) 133-156.
12. J. Kolafa and I. Nezbeda, *Mol. Phys.* **61** (1987) 161-175.
13. I. Nezbeda and G. A. Iglesia-Silva, *Mol. Phys.* **69** (1990) 767-774.
14. I. Nezbeda and J. Pavlicek, *Fluid Phase Equilibria*, **116** (1996) 530-536.
15. R. Aris, G. R. Gavalas, *Phil. Trans. R. Soc. London A* **260** (1966) 351~393.
16. J. A. Gualtieri, J. M. Kincaid, G. Morrison, *J. Chem. Phys.* **77** (1982) 521~536.
17. R. L. Cotterman and J. M. Prausnitz, in G. Astarita and S. I. Sandler (Eds.) *Kineticc and Thermodynamic Lumping of Multicomponent Mixtures*, Elsevier, Amsterdam, 1991, pp 229-275.
18. H. Kehlen, M. T. Ratzsch and J. Bergmann, *J. Macromol. Sci.-Chem.*, **A 24** (1987) 1-16.
19. S. Beerbaum, J. Bergmann, H. Kehlen and M. T. Ratzsch, *J. Macromol. Sci.-Chem.*, **A 24** (1987) 1445-1463.
20. Y. Hu, X. Ying, D. T. Wu and J. M. Prausnitz, *Macromolecules*, **26** (1993) 6817-6823.
21. Y. Hu, X. Ying, D. T. Wu and J. M. Prausnitz, *Fluid Phase Equilibria*, **98** (1994) 113-128.
22. Y. Hu, X. Ying, D. T. Wu and J. M. Prausnitz, *Fluid Phase Equilibria*, **104** (1995) 229-252.
23. R. L. Cotterman, R. Bender and J. M. Prausnitz, *Ind. Eng. Chem. Process Des. Dev.*, **24** (1985) 194-203.
24. D. Browarzik and H. Kehlen, *Fluid Phase Equilibria*, **123** (1996) 17-28.
25. Y. Hu and X. Ying, *Fluid Phase Equilibria*, **127** (1997) 21-27.
26. Y. Hu and J. M. Prausnitz, *Fluid Phase Equilibria*, **130** (1997) 1-18.
27. D. Browarzik, M. Kowalewski and H. Kehlen, *Fluid Phase Equilibria*, **142** (1998) 149-162.
28. R. A. Heidemann, *Fluid Phase Equilibria*, **14** (1983) 55-78.

Figure captions

Fig. 1 Transition from Type II to Type III.

$$T_K^c = 400\text{K}, V_K^c = 2 \times 10^{-4} \text{m}^3 \cdot \text{mol}^{-1}, a^{(0)} = 0.2804 \text{Pa}^{0.5} \cdot \text{m}^3 \cdot \text{mol}^{-1}, a^{(1)} = 0.01417 \text{Pa}^{0.5} \cdot \text{m}^3 \cdot \text{g}^{-1},$$

$$b^{(0)} = 8.978 \times 10^{-6} \text{m}^3 \cdot \text{mol}^{-1}, b^{(1)} = 6.009 \times 10^{-7} \text{m}^3 \cdot \text{g}^{-1}, k_d = -0.1067.$$

$$\mu_{(2)} = 347 \text{g}^2 \cdot \text{mol}^{-2}; 1: \bar{M} = 72 \text{g} \cdot \text{mol}^{-1}, 2: \bar{M} = 81.4 \text{g} \cdot \text{mol}^{-1}, 3: \bar{M} = 88 \text{g} \cdot \text{mol}^{-1}$$

dotted line: vapor-pressure line of pure discrete component, solid line: critical-point loci

Fig 2. Type IV Critical Loci (line 1 in figure 3).

$$T_K^c = 600\text{K}, V_K^c = 2 \times 10^{-4} \text{m}^3 \cdot \text{mol}^{-1}, a^{(0)} = 0.2804 \text{Pa}^{0.5} \cdot \text{m}^3 \cdot \text{mol}^{-1},$$

$$a^{(1)} = 0.01847 \text{Pa}^{0.5} \cdot \text{m}^3 \cdot \text{g}^{-1},$$

$$b^{(0)} = 8.978 \times 10^{-6} \text{m}^3 \cdot \text{mol}^{-1}, b^{(1)} = 6.009 \times 10^{-7} \text{m}^3 \cdot \text{g}^{-1}, k_d = -0.1723.$$

solid line: critical loci ; dotted line: vapor pressure.

Fig. 3 Transition from Type IV to Type III (Enlargement near C).

$$\bar{M} = 96 \text{g} \cdot \text{mol}^{-1}; 1. \delta\text{-distribution}(\mu_{(2)} = 0), 2. \mu_{(2)} = 35 \text{g}^2 \cdot \text{mol}^{-2}, 3. \mu_{(2)} = 80 \text{g}^2 \cdot \text{mol}^{-2},$$

solid line: critical loci ; dotted line: vapor pressure. Parameters see caption of Fig.2.

Fig. 4 Distribution Function of the Homologue Corresponding to Fig. 3.

$$\bar{M} = 96 \text{g} \cdot \text{mol}^{-1}; 1. \text{Dirac } \delta\text{-distribution}(\mu_{(2)} = 0), 2. \mu_{(2)} = 35 \text{g}^2 \cdot \text{mol}^{-2}, 3. \mu_{(2)} = 80 \text{g}^2 \cdot \text{mol}^{-2}.$$

Fig. 5 Transition from Type II to Type IV.

$$\bar{M} = 96 \text{g} \cdot \text{mol}^{-1}, 1. \mu_{(2)} = 0, 2. \mu_{(2)} = 347 \text{g}^2 \cdot \text{mol}^{-2}, 3. \mu_{(2)} = 800 \text{g}^2 \cdot \text{mol}^{-2}$$

$$T_K^c = 600\text{K}, V_K^c = 2 \times 10^{-4} \text{m}^3 \cdot \text{mol}^{-1}, a^{(0)} = 0.2804 \text{Pa}^{0.5} \cdot \text{m}^3 \cdot \text{mol}^{-1},$$

$$a^{(1)} = 0.01699 \text{Pa}^{0.5} \cdot \text{m}^3 \cdot \text{g}^{-1},$$

$$b^{(0)} = 8.978 \times 10^{-6} \text{m}^3 \cdot \text{mol}^{-1}, b^{(1)} = 6.009 \times 10^{-7} \text{m}^3 \cdot \text{g}^{-1}, k_d = -0.1267.$$

solid line: loci of critical point ; dotted line: vapor pressure.

Fig. 6 Enlargement of the Region near C in Fig. 5 .

solid line: 1. type II, dotted line: 2. type IV, dash-dot line: 3. type IV.

Fig. 7 Transition from Type II to Type IV, then to Type III.

$$T_K^c = 600\text{K}, V_K^c = 2 \times 10^{-4} \text{m}^3 \cdot \text{mol}^{-1}, a^{(0)} = 0.2804 \text{Pa}^{0.5} \cdot \text{m}^3 \cdot \text{mol}^{-1},$$

$$a^{(1)} = 0.01699 \text{Pa}^{0.5} \cdot \text{m}^3 \cdot \text{g}^{-1},$$

$$b^{(0)} = 8.978 \times 10^{-6} \text{m}^3 \cdot \text{mol}^{-1}, b^{(1)} = 6.009 \times 10^{-7} \text{m}^3 \cdot \text{g}^{-1}, \mu_{(2)} = 800 \text{g}^2 \cdot \text{mol}^{-2}, k_d = -0.1267.$$

solid line: critical-point loci; dotted line: vapor pressure.

Fig. 8 Distribution Function of the Homolog Corresponding to Fig. 7.

$$\mu_{(2)} = 800 \text{g}^2 \cdot \text{mol}^{-2}; 1. \bar{M} = 72 \text{g} \cdot \text{mol}^{-1}; 2. \bar{M} = 96 \text{g} \cdot \text{mol}^{-1}; 3. \bar{M} = 104 \text{g} \cdot \text{mol}^{-1};$$

$$4. \bar{M} = 112 \text{g} \cdot \text{mol}^{-1}$$

Fig 9 Transition from Type I to Type V.

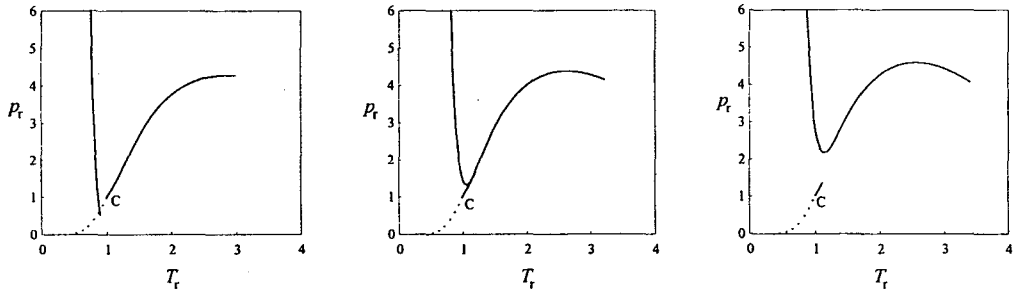
$$\bar{M} = 96 \text{g} \cdot \text{mol}^{-1}, 1. \mu_{(2)} = 0, 2. \mu_{(2)} = 100 \text{g}^2 \cdot \text{mol}^{-2}, 3. \mu_{(2)} = 347 \text{g}^2 \cdot \text{mol}^{-2}, 4. \mu_{(2)} = 600 \text{g}^2 \cdot \text{mol}^{-2}$$

$$T_K^c = 600\text{K}, V_K^c = 3 \times 10^{-4} \text{m}^3 \cdot \text{mol}^{-1}, a^{(0)} = 0.2804 \text{Pa}^{0.5} \cdot \text{m}^3 \cdot \text{mol}^{-1},$$

$$a^{(1)} = 0.02253 \text{Pa}^{0.5} \cdot \text{m}^3 \cdot \text{g}^{-1},$$

$$b^{(0)} = 8.978 \times 10^{-6} \text{m}^3 \cdot \text{mol}^{-1}, b^{(1)} = 9.481 \times 10^{-7} \text{m}^3 \cdot \text{g}^{-1}.$$

Fig. 10 Enlargement of the Region near C in Fig. 9.



(a)

(b)

(c)

Fig. 1 Transition from Type II to Type III.

$$T_K^c = 400\text{K}, V_K^c = 2 \times 10^{-4} \text{m}^3 \cdot \text{mol}^{-1}, a^{(0)} = 0.2804 \text{Pa}^{0.5} \cdot \text{m}^3 \cdot \text{mol}^{-1}, a^{(1)} = 0.01417 \text{Pa}^{0.5} \cdot \text{m}^3 \cdot \text{g}^{-1},$$

$$b^{(0)} = 8.978 \times 10^{-6} \text{m}^3 \cdot \text{mol}^{-1}, b^{(1)} = 6.009 \times 10^{-7} \text{m}^3 \cdot \text{g}^{-1},$$

$$k_d = -0.1067.$$

$$\mu_{(2)} = 347 \text{g}^2 \cdot \text{mol}^{-2}; 1: \bar{M} = 72 \text{g} \cdot \text{mol}^{-1}, 2: \bar{M} = 81.4 \text{g} \cdot \text{mol}^{-1}, 3: \bar{M} = 88 \text{g} \cdot \text{mol}^{-1}$$

dotted line: vapor-pressure line for pure discrete component; solid line: critical-point loci.

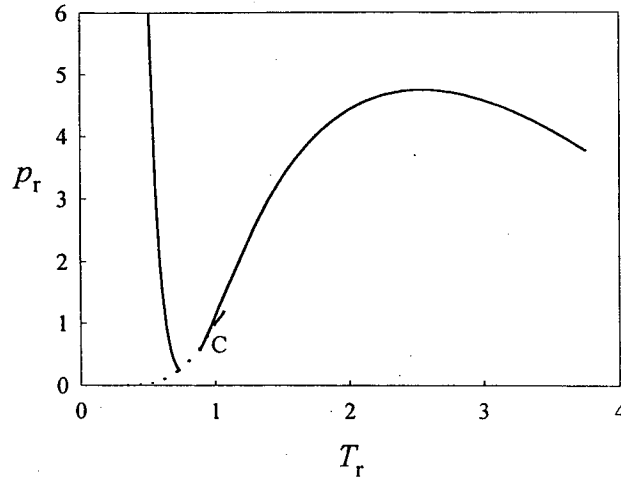


Fig 2. Type IV Critical Loci (line 1 in figure 3).

$$T_K^c = 600\text{K}, V_K^c = 2 \times 10^{-4} \text{m}^3 \cdot \text{mol}^{-1}, a^{(0)} = 0.2804 \text{Pa}^{0.5} \cdot \text{m}^3 \cdot \text{mol}^{-1}, a^{(1)} = 0.01847 \text{Pa}^{0.5} \cdot \text{m}^3 \cdot \text{g}^{-1},$$

$$b^{(0)} = 8.978 \times 10^{-6} \text{m}^3 \cdot \text{mol}^{-1}, b^{(1)} = 6.009 \times 10^{-7} \text{m}^3 \cdot \text{g}^{-1},$$

$$k_d = -0.1723.$$

solid line: critical loci ; dotted line: vapor pressure.

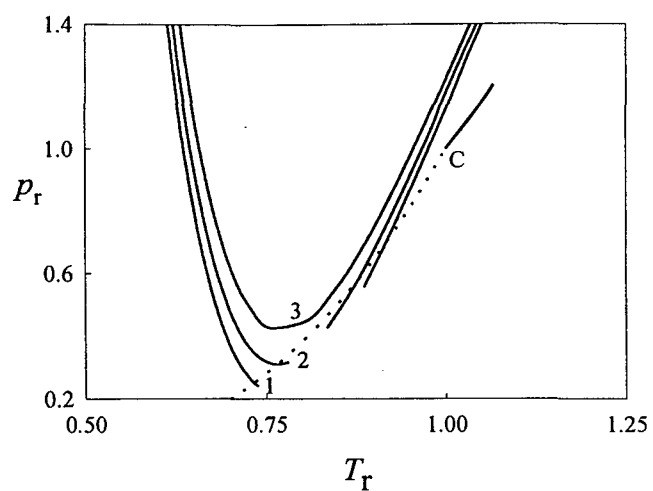


Fig. 3 Transition from Type IV to Type III (Enlargement near C).
 $\bar{M}=96 \text{ g}\cdot\text{mol}^{-1}$; 1. δ -distribution($\mu_{(2)}=0$), 2. $\mu_{(2)}=35 \text{ g}^2\cdot\text{mol}^{-2}$, 3. $\mu_{(2)}=80 \text{ g}^2\cdot\text{mol}^{-2}$,
 solid line: critical loci ; dotted line: vapor pressure. Parameters as in Fig.2.

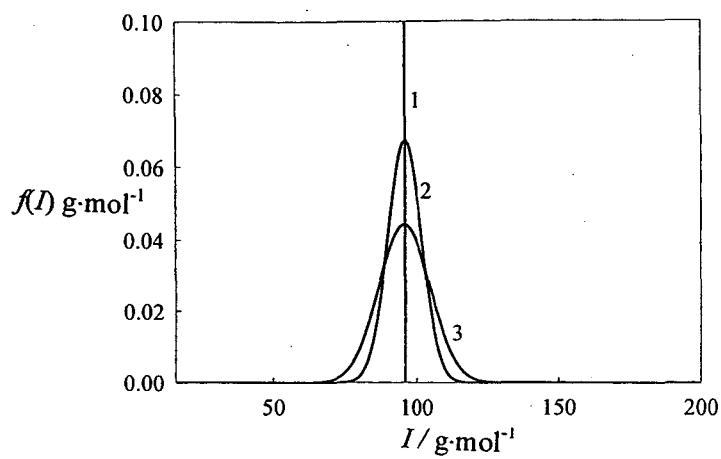


Fig. 4 Distributions function for the Homologue Corresponding to Fig. 3.
 $\bar{M} = 96 \text{ g}\cdot\text{mol}^{-1}$; 1. Dirac δ -distribution ($\mu_{(2)} = 0$), 2. $\mu_{(2)} = 35 \text{ g}^2\cdot\text{mol}^{-2}$, 3. $\mu_{(2)} = 80 \text{ g}^2\cdot\text{mol}^{-2}$.

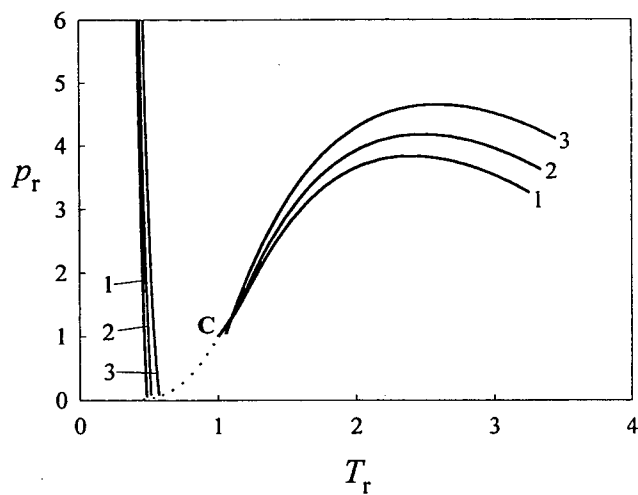


Fig. 5 Transition from Type II to Type IV.

$\bar{M}=96 \text{ g}\cdot\text{mol}^{-1}$, 1. $\mu_{(2)}=0$, 2. $\mu_{(2)}=347 \text{ g}^2\cdot\text{mol}^{-2}$, 3. $\mu_{(2)}=800 \text{ g}^2\cdot\text{mol}^{-2}$
 $T_K^c=600\text{K}$, $V_K^c=2\times 10^{-4} \text{ m}^3\cdot\text{mol}^{-1}$, $a^{(0)}=0.2804 \text{ Pa}^{0.5}\cdot\text{m}^3\cdot\text{mol}^{-1}$, $a^{(1)}=0.01699 \text{ Pa}^{0.5}\cdot\text{m}^3\cdot\text{g}^{-1}$,
 $b^{(0)}=8.978\times 10^{-6} \text{ m}^3\cdot\text{mol}^{-1}$, $b^{(1)}=6.009\times 10^{-7} \text{ m}^3\cdot\text{g}^{-1}$, $k_d=-0.1267$.
 solid line: loci of critical point ; dotted line: vapor pressure.

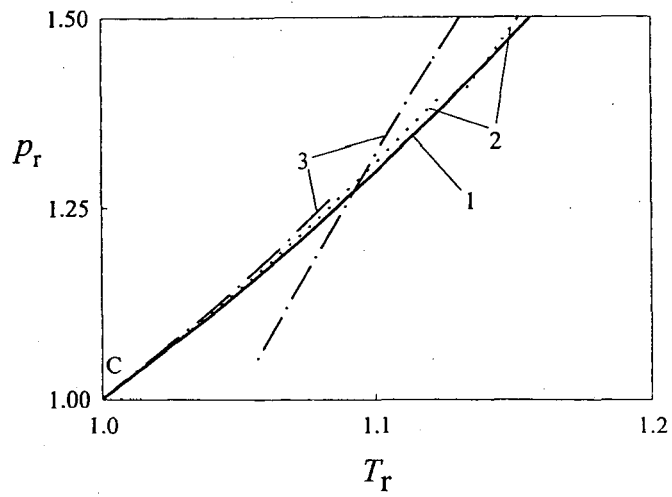
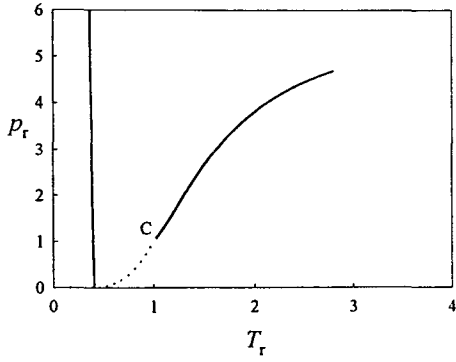
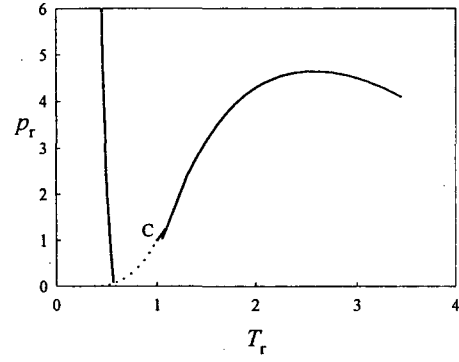


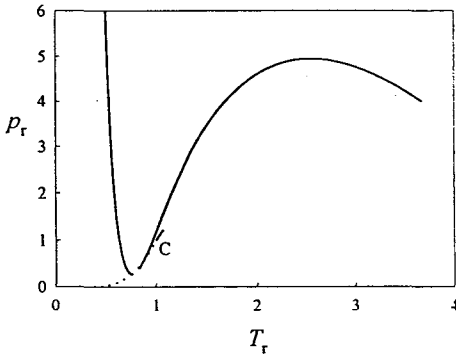
Fig. 6 Enlargement of the Region near C in Fig. 5 .
solid line: 1. type II; dotted line: 2. type IV; dash-dot line: 3. type IV.



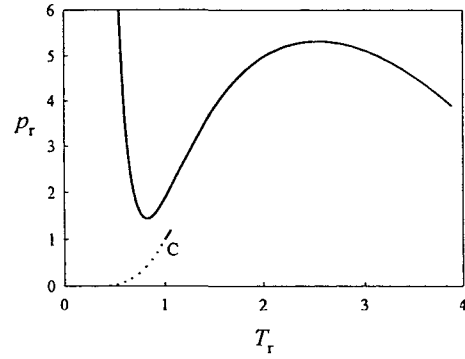
(a) $\bar{M}=72 \text{ g}\cdot\text{mol}^{-1}$, type II .



(b) $\bar{M}=96 \text{ g}\cdot\text{mol}^{-1}$, type IV.



(c) $\bar{M}=104 \text{ g}\cdot\text{mol}^{-1}$, type IV .



(d) $\bar{M}=112 \text{ g}\cdot\text{mol}^{-1}$, type III.

Fig. 7 Transition from Type II to Type IV, then to Type III.

$T_K^c=600\text{K}$, $V_K^c=2\times 10^{-4}\text{m}^3\cdot\text{mol}^{-1}$, $a^{(0)}=0.2804\text{Pa}^{0.5}\cdot\text{m}^3\cdot\text{mol}^{-1}$, $a^{(1)}=0.01699\text{Pa}^{0.5}\cdot\text{m}^3\cdot\text{g}^{-1}$,
 $b^{(0)}=8.978\times 10^{-6}\text{m}^3\cdot\text{mol}^{-1}$, $b^{(1)}=6.009\times 10^{-7}\text{m}^3\cdot\text{g}^{-1}$, $\mu_{(2)}=800 \text{ g}^2\cdot\text{mol}^{-2}$, $k_d=-0.1267$.

solid line: critical-point loci; dotted line: vapor pressure.

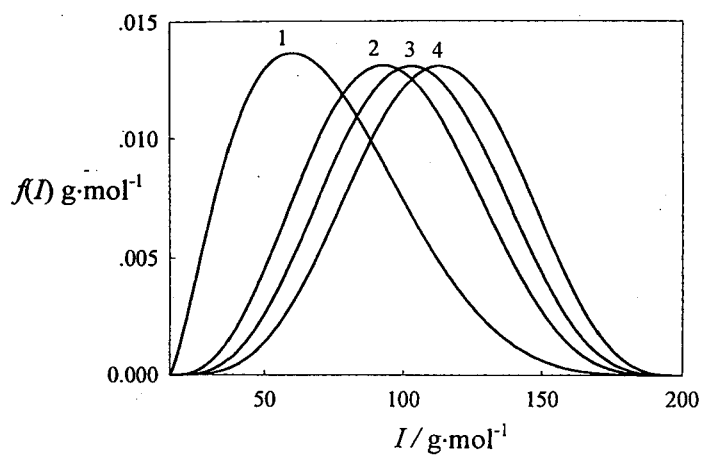


Fig. 8 Distribution of the Homologue Corresponding to Fig. 7.
 $\mu_{(2)} = 800 \text{ g}^2 \cdot \text{mol}^{-2}$; 1. $\bar{M} = 72 \text{ g}\cdot\text{mol}^{-1}$; 2. $\bar{M} = 96 \text{ g}\cdot\text{mol}^{-1}$; 3. $\bar{M} = 104 \text{ g}\cdot\text{mol}^{-1}$; 4. $\bar{M} = 112 \text{ g}\cdot\text{mol}^{-1}$

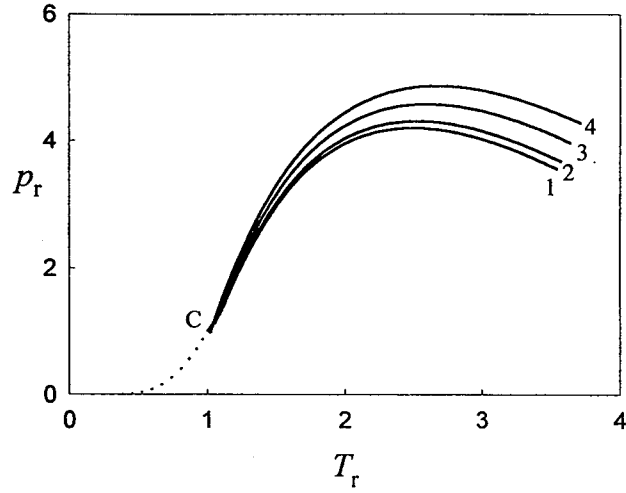


Fig 9 Transition from Type I to Type V.

$$\begin{aligned} \bar{M} &= 96 \text{g} \cdot \text{mol}^{-1}, 1. \mu_{(2)} = 0, 2. \mu_{(2)} = 100 \text{g}^2 \cdot \text{mol}^{-2}, 3. \mu_{(2)} = 347 \text{g}^2 \cdot \text{mol}^{-2}, 4. \mu_{(2)} = 600 \text{g}^2 \cdot \text{mol}^{-2} \\ T_K^c &= 600 \text{K}, V_K^c = 3 \times 10^{-4} \text{m}^3 \cdot \text{mol}^{-1}, a^{(0)} = 0.2804 \text{Pa}^{0.5} \cdot \text{m}^3 \cdot \text{mol}^{-1}, a^{(1)} = 0.02253 \text{Pa}^{0.5} \cdot \text{m}^3 \cdot \text{g}^{-1}, \\ b^{(0)} &= 8.978 \times 10^{-6} \text{m}^3 \cdot \text{mol}^{-1}, b^{(1)} = 9.481 \times 10^{-7} \text{m}^3 \cdot \text{g}^{-1}. \end{aligned}$$

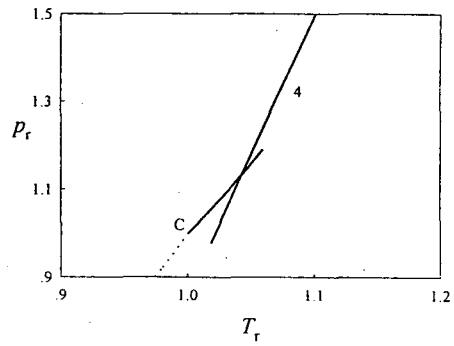
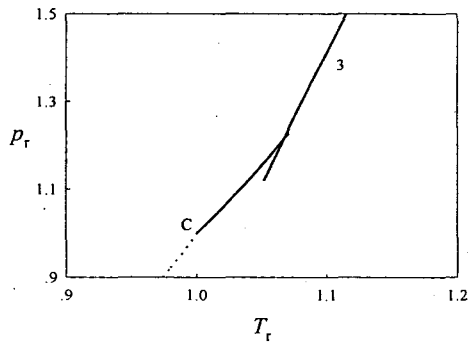
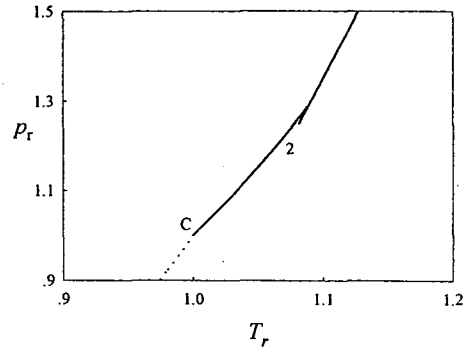
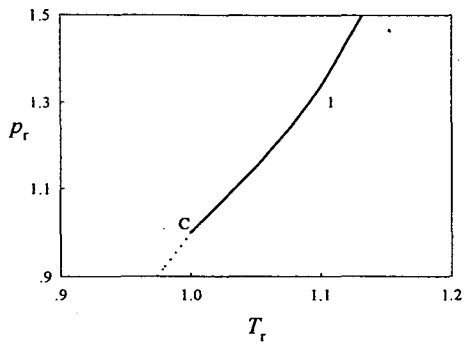


Fig. 10 Enlargement of the Region near C in Fig. 9.

ERNEST ORLANDO LAWRENCE BERKELEY NATIONAL LABORATORY
ONE CYCLOTRON ROAD BERKELEY, CALIFORNIA 94720

ABT710



LBL Libraries